Retaining an Upper Bound for the Capillary Retention of Two-Phase Flow in Porous Media

Transport in Porous Media (2022) 143:639–656
https://doi.org/10.1007/s11242-022-01802-7

ORIGINAL RESEARCH PAPER

Retaining an Upper Bound for the Capillary Retention of Two-Phase Flow in Porous Media

Al Yaqathan Al Ghafri[1] · **Eric Mackay**[1] · **Karl Stephen**[1]

Received: 23 June 2021 / Accepted: 18 May 2022 / Published online: 21 June 2022

Abstract
At the sub-meter scale, capillary retention occurs when two immiscible phases flow across two heterogeneous media. It happens in the upstream medium, and the phase retained depends on the heterogeneity order and the system wettability. This phenomenon has a major impact on the oil recovery and hence requires comprehension. The analysis of the spatial variation in the phase saturation along the flowing domain is well established. However, the literature lacks the general characteristics of capillary retention caused by such variation at various flowing conditions. The continuum model for the flow of two immiscible phases in porous media at steady-state conditions is examined. The analysis is limited to the medium with a single discontinuity in rock properties. In this examination, the characteristics of the capillary retention upstream of the discontinuity are the primary consideration. Three retention regions related to the flow regime are identified: two plateaus and a transition zone occurring, in general, at intermediate capillary number. The width and location of the transition depend on the fractional flow. The crucial finding is related to the identification of an upper bound for the capillary retention and its dependency on the capillary variable ratio and the form of the Leverett *J*-curve. Two *J*-models are investigated, and it is shown that, for a given capillary variable ratio, the upper bound depends on the level of flatness of the *J*-curve at intermediate saturations. Potential implications of the current analysis to reservoir characterization are also discussed.

Article Highlights
- Three retention regions related to the ow regime are identified: two plateaus and a transition zone occurring at intermediate capillary numbers. The width and position of the transition depend on the fractional flow.
- An upper bound for the capillary retention is derived and its dependency on the heterogeneity ratio and the form of the Leverett-J curve is discussed..
- Potential implication to reservoir characterization: In the case of steeper Leverett-J curves with low to moderate random heterogeneity ratios, the upper bound is minimal regardless of the various lithologies and their congurations. In such conditions, the upper bound can be used to assert the insignicance of the eld-scale capillary retention.

Keywords Capillary retention · Capillary continuity · Steady-state · Upper bound · Capillary number

Extended author information available on the last page of the article

1 Introduction

At the continuum scale, reservoir heterogeneity can cause various forms of phase retention. An example of this type includes bypassed oil relative to the Buckley–Leverett displacement, during the secondary recovery of oil by displacement process, due to the immiscible viscous fingering mechanism, which manifests itself due to small-scale perturbations and grows into large scale fingers. This form of retention causes a significant amount of unswept and uncontacted oil. Another form of retention occurs when two immiscible fluids flow across two discontinuous media under capillary pressure. This latter form causes retention of one of the phases, depending on the heterogeneity order and the medium wettability. It has attained the interest of numerous investigators over the past four decades (Yortsos and Chang 1990; Chang and Yortsos 1992; Dale et al. 1994; Duijn et al. 1995; van Duijn and de Neef 1998; Debbabi et al. 2017). It is evident that capillary forces cause phase retention on various scales, and this mechanism is very different from the well-known *pore-scale capillary trapping* (Bear 1975; Blunt 2017). The need for a detailed understanding of this mechanism comes from the fact that capillary pressure and heterogeneity are regarded as intrinsic properties of immiscible fluids and the reservoir rocks. The latter's scale exhibits *a hierarchical nature* depending on the process and environment of deposition (Miall 2006; Reading 2009). The capillary retention, in general, operates at the *bedding/lamination* scale where the capillary force is significant (Ekrann et al. 1996).

The analytical results regarding the spatial variation of saturation and capillary pressure in a discontinuous porous medium under *steady-state* conditions are attributed to (Yortsos and Chang 1990; Chang and Yortsos 1992; Dale et al. 1994; Duijn et al. 1995; van Duijn and de Neef 1998). The first experimental evidence for the capillary retention is accredited to (Ledeboer 1992). This evidence might address the plausibility of using the statically developed *constitutive equations* namely: capillary pressure and Leverett equations for dynamic conditions.

The general statement of the problem is based on the fractional flow formalism derived from a system of governing flow equations namely: the continuity, momentum, and two supplementary equations. The momentum equation, Darcy's law, assumes a low Reynolds number and it relates the phase velocity (kinematic quantity) to the phase pressure (kinetic quantity). From the system of equations, the fractional flow equation is derived which describes the retention mechanism in a discontinuous medium. The unsteady-state retention is of interest to us but that requires understanding the steady-state retention, the subject of this article, since the former state can be seen locally, in space, as a steady state in a given time.

In this article, we will characterize capillary retention under various capillary numbers, fractional flow, and J-curves at steady state. More attention is paid to the boundedness property of capillary retention and its dependency on various parameters.

1.1 Problem Formulation

Consider the incompressible flow of water and oil through a one-dimensional porous medium with porosity $\phi = \phi(x)$ and permeability $\hat{k} = \hat{k}(x)$. The two-phase flow is governed by the system, (Bear 1975)

$$\phi \frac{\partial \hat{S}_i}{\partial \hat{t}} + \frac{\partial \hat{u}_i}{\partial \hat{x}} = 0 \tag{1.1}$$

$$\hat{u}_i = -\hat{\lambda}_i \hat{k} \frac{\partial \hat{p}_i}{\partial \hat{x}} \tag{1.2}$$

$$\hat{S}_w + \hat{S}_o = 1 \tag{1.3}$$

$$\hat{p}_o - \hat{p}_w = \hat{p}_c \tag{1.4}$$

where the subscript i denotes either water phase (w) or oil phase (o). The variables $\hat{S}_i, \hat{\lambda}_i, \hat{u}_i, \hat{p}_i$ are saturation, mobility, Darcy velocity and pressure of the phase i, respectively. We define the residual saturations, $\hat{S}_{wr}(x)$ and $\hat{S}_{or}(x)$, to be the saturation at which $\hat{\lambda}_w(\hat{S}_{wr}) = 0$ and $\hat{\lambda}_o(1 - \hat{S}_{or}) = 0$, respectively, i.e. the phase becomes immobile. The domain of the phase mobility functions is defined over the interval $[\hat{S}_{wr}, 1 - \hat{S}_{or}]$ and the difference between these end-points is the movable oil saturation, $\hat{S}_{om} = 1 - \hat{S}_{wr} - \hat{S}_{or}$. Also, the maximum values of $\hat{\lambda}_w$ and $\hat{\lambda}_o$ occur at $\hat{\lambda}_w^o = \hat{\lambda}_w(1 - \hat{S}_{or})$ and $\hat{\lambda}_o^o = \hat{\lambda}_o(\hat{S}_{wr})$, respectively. The variable $\hat{p}_c$ given by Eq. (1.4) is the capillary pressure and is a function of ϕ, $\hat{k}$ and $\hat{S}_w$. To put the governing flow equations in the dimensionless form, we define the variables

$$x = \frac{\hat{x}}{L} \tag{1.5}$$

$$t = \frac{u_t \hat{t}}{L} \tag{1.6}$$

$$u_i = \frac{\hat{u}_i}{u_t} \tag{1.7}$$

$$S_i = \frac{\hat{S}_i - \hat{S}_{ir}}{\hat{S}_{om}} = \frac{\hat{S}_i - \hat{S}_{ir}}{1 - \hat{S}_{wr} - \hat{S}_{or}} \tag{1.8}$$

$$p_i = \frac{\hat{\lambda}_o^o \bar{\hat{k}} \hat{p}_i}{u_t L} \tag{1.9}$$

$$\lambda_i = \frac{\hat{\lambda}_i}{\hat{\lambda}_i^o} \tag{1.10}$$

$$M_e = \frac{\hat{\lambda}_w^o}{\hat{\lambda}_o^o} \tag{1.11}$$

$$k = \frac{\hat{k}}{\bar{\hat{k}}} \tag{1.12}$$

$$p_c = \frac{\hat{p}_c}{\sigma_{ow} cos\theta \sqrt{\bar{\hat{k}}}} = \frac{J}{\tau} \tag{1.13}$$

$$\tau = \left(\frac{k}{\phi}\right)^{\frac{1}{2}} \tag{1.14}$$

where L, u_t, $\bar{\hat{k}}$, M_e and J are length of the flow domain, injection velocity, average permeability, end-point mobility ratio and Leverett J-function, respectively. The Leverett relationship, Eq. (1.13), is used to define the characteristic pressure for $p_c(S_w, \tau)$ where the variable τ defined by Eq. (1.14) is referred to as the capillary variable (Leverett et al. 1942; Yortsos and Chang 1990). The capillary variable is correlated with the pore size of the medium. In general, low τ dictates small pore size in fine medium and high τ large pore size in coarse medium. The characteristic time is the time required to inject a total volume equal to the bulk volume and so the time defined in (1.6) is measured in unit bulk volume. The characteristic pressure is the pressure drop across the medium with an average permeability when oil is the only phase flowing. Using the new variables, the system of Eqs. (1.1–1.4) can be recast into the dimensionless system

$$\phi \hat{S}_{om} \frac{\partial S_i}{\partial t} + \frac{\partial u_i}{\partial x} = 0 \tag{1.15}$$

$$u_w = -M_e \lambda_w k \frac{\partial p_w}{\partial x}, \quad u_o = -\lambda_o k \frac{\partial p_o}{\partial x} \tag{1.16}$$

$$S_w + S_o = 1 \tag{1.17}$$

$$p_o - p_w = \gamma p_c \tag{1.18}$$

where the parameter γ is defined as

$$\gamma = \frac{\lambda_o^o \sigma_{ow} cos\theta \sqrt{\bar{\hat{k}}}}{u_t L} \tag{1.19}$$

is the capillary number, (Yortsos and Chang 1990; Chang and Yortsos 1992).

Taking the sum of two continuity equations, (1.15), in both phases and using (1.17), to eliminate S_w and S_o gives the divergence form $\frac{\partial u}{\partial x} = 0$ where $u = u_w + u_o = 1$ is the total velocity. This implies that the *dimensional* total velocity $\hat{u}$ is constant and equal to the injection velocity u_t. The divergence form along with Eqs. (1.16) and (1.18) is used to substitute for u_o, p_o and p_w to give the *fractional flow* of water

$$u_w(x,t) = f_w + \gamma f_w \lambda_o k \frac{\partial p_c}{\partial x} \tag{1.20}$$

where

$$f_w(S_w) = \frac{M_e \lambda_w}{M_e \lambda_w + \lambda_o} \tag{1.21}$$

is, by definition, the *viscous limit* fractional flow of water occurring when $\gamma \to 0$. Using Eqs. (1.13) and (1.14) to expand the capillary pressure gradient, the fractional flow equation becomes

$$u_w(x,t) = f_w - \gamma\phi\left(h\tau\frac{\partial S_w}{\partial x} + g\frac{d\tau}{dx}\right) \tag{1.22}$$

where

$$h(S_w) = -f_w\lambda_o J', \quad g(S_w) = f_w\lambda_o J \tag{1.23}$$

where the prime denotes the derivative with respect to S_w . A water-wet medium is assumed which implies that $J(S_w) \geq 0$. We also require that $\lim_{S_w \to 0} J = +\infty$ and $J(1) = 0$. In the continuity equation for water phase, we shall consider steady-state conditions which implies that $0 \leq u_w \leq 1$ is constant along the flow domain. Hence, the argument u_w, along with γ, is considered parameters in Eq. (1.22) and the partial derivative is replaced by the normal derivative since x is the only variable argument of S_w . We shall also consider a single discontinuity at x_0 in which ϕ and $k = k(\phi)$, and hence τ are represented by step functions. Various models have been proposed to model permeability but we choose here porosity to be the sole argument of permeability (Kozeny 1927; Carman 1937; Tixier 1949; Wyllie and Rose 1950; Timur 1968; Coates and Dumanoir 1973; Amaefule et al. 1993). On either side of the step (discontinuity), Eq. (1.22) is well-posed and reduces to

$$\frac{dS}{dx} = F(S) = \left(\frac{1}{\gamma\phi\tau}\right)\frac{f-u}{h}, \quad x \neq x_0. \tag{1.24}$$

For shorthand, we have dropped the subscript (w) from the saturation variable and the saturation-dependent functions since water is the only phase involved in the above equation. On either side of the discontinuity, the function F is Lipschitz continuous which implies the existence and uniqueness of the solution S (Howlett and Henrici 1966; Bramwell and Kreyszig 1979).

Similar to k, we assume that $\hat{S}_{wr} = \hat{S}_{wr}(\phi)$ and $\hat{S}_{or}$ is constant for the whole medium. The solution is obtained numerically from slope field F for a given initial condition. The jump in the solution at x_0 is governed by the continuity of capillary pressure postulate which will be discussed later. Given the solution, we shall investigate the retention under various capillary numbers, fractional flow ranges, and J–curves.

2 Model Description and Methodology

2.1 Model Description

We define the capillary retention to be the saturation retained upstream of the discontinuity at x_0. We choose a unit flow domain with $x_0 \in [0,1]$ and ϕ and $k(\phi)$ are given by step functions. With these choices and since ϕ is constant in $[[0, x_0]$, the capillary retention is quantified as

$$\hat{\kappa} = \frac{1}{x_0}\int_0^{x_0} \Delta\hat{S}\, dx \tag{2.1}$$

where $\Delta\hat{S} = \hat{S} - \hat{S}_v$ and $\hat{S}_v$ is the viscous limit saturation solution. The fact $\Delta\hat{S} = \hat{S}_{om}\Delta S$ implies that $\hat{\kappa}$ is directly proportional to $\hat{S}_{om}$ for given ΔS which is intuitive. The subtlety is in the relationship between $\hat{\kappa}$ and ΔS for given $\hat{S}_{om}$ which requires exploration. For this purpose and since $\hat{S}_{om}$ is constant in $[[0, x_0]$, we define the normalized capillary retention

$$\kappa = \frac{\hat{\kappa}}{\hat{S}_{om}} = \frac{1}{x_0}\int_0^{x_0} \Delta S\, dx. \tag{2.2}$$

The definition implies a water retention if $S > S_v$ and oil retention if $S < S_v$. We assume phase mobilities of the form

$$\lambda_w(S) = (S)^4, \quad \lambda_o(S) = (1-S)^2 \tag{2.3}$$

and are plotted in Fig. 1. We choose an end-point mobility ratio of $M_e = 160$, typical for viscous oil reservoirs. From the phase mobilities and end-point mobility ratio, the fractional flow is computed and plotted in Fig. 1. The J-function given by the form, (van Genuchten 1980):

$$J(S) = \frac{1}{q}\left((S)^{-\frac{1}{m}} - 1\right)^{\frac{1}{n}} \tag{2.4}$$

is parametrized by a scaling factor q related to the *average* pore size distribution and m and n which are also related to the pore size distribution of the porous medium. For $n(m) = 1$, the J-function corresponds to the Brooks and Corey model, BC, for shorthand, and to Van Genuchten–Burdine model, VB, if $n(m) = \frac{2}{1-m}$ (Brooks and Corey 1966; van Genuchten

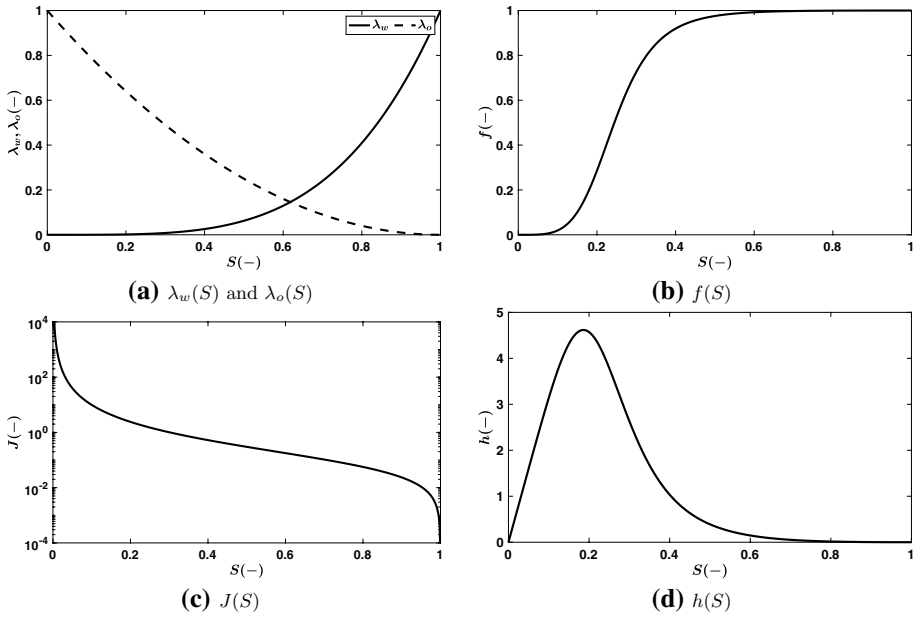

Fig. 1 (**a**) Plots of various saturation-dependent functions. The phase mobilities are given by (2.2) . The viscous dominated fractional flow is given by (1.15) with $M_e = 160$. (**b**) The Leverett J-function is given by BC model with $n = 1$ in (2.3). The diffusivity function is given by (1.17)

1980). Figure 1c and d shows the $J(S)$ and $h((S)$ functions using BC model with $q = 10$ and $m = \frac{1}{2}$. We shall, for simplicity, fix the porosity and permeability, the phase mobilities, end-point mobility ratio. With this consideration, $\kappa = \kappa(u, \gamma)$.

The capillary variable function is given by:

$$\tau(x) = \Delta\tau H(x - x_0) + \tau^- \tag{2.5}$$

where $\Delta\tau = \tau^+ - \tau^-$ is the difference in the downstream and upstream capillary variable values and $H(x)$ is the Heaviside function defined as:

$$H(x) = \begin{cases} 0 & \text{if } 0 \geq x \geq x_0 \\ 1 & \text{if } x_0 > x \geq 1 \end{cases}. \tag{2.6}$$

For the calculation of τ we choose $\phi^- = 0.1$, $\phi^+ = 0.3$, $k(\phi^-) = 0.1$ and $k(\phi^+) = 1.2$ These data give $\tau^- = 1$ and $\tau^+ = 2$. The discontinuity is positioned at $x_0 = 0.50$. We shall consider two cases for the analysis of capillary retention: ascending and descending capillary variable.

2.2 Numerical Scheme

Consider the initial value problem:

$$F(S) = \left(\frac{1}{\gamma\phi^-\tau^-}\right)\frac{f(S) - u}{h(S)}, \quad S(1) = S_v \tag{2.7}$$

in the interval [0, 1]. The solution is constructed numerically using the finite difference Runge–Kutta method and given by:

$$S = \begin{cases} S^+ = f^{-1}(u) & \text{if } 1 \geq x \geq x_0 \\ S^- + \Delta x \sum_{i=0}^{k} \bar{\psi}_i & \text{if } x_0 > x_k \geq 0 \end{cases} \tag{2.8}$$

where $S^+ = S_v$, $S^- = S(x_0)$ and

$$\bar{\psi}_i(S_i, \Delta x) = \frac{1}{6}\left(\psi_{i1} + 2(\psi_{i2} + \psi_{i3}) + \psi_{i4})\right) \tag{2.9}$$

$$\psi_{i1} = F(S_i), \quad \psi_{i2} = F(S_i + \frac{\Delta x}{2}\psi_{i1}) \tag{2.10}$$

$$\psi_{i3} = F(S_i + \frac{\Delta x}{2}\psi_{i2}), \quad \psi_{i4} = F(S_i + \Delta x\psi_{i3}) \tag{2.11}$$

To the upstream of the discontinuity, the solution approaches the *upstream saturation* S^-. To the downstream of the discontinuity, the solution is constant and referred as the *downstream saturation* S^+. The upstream saturation is S^- at x_0 which is related to the downstream saturation by the continuity of capillary pressure at x_0. The general behaviour of the solution at and on either side of the discontinuity is well established (Yortsos and Chang 1990; Chang and Yortsos 1992; Dale et al. 1994; Duijn et al. 1995; van Duijn and de Neef 1998). The solution is constructed backwards as the following:

- At $x \in (x_0, 1]$, the unique solution is identical to that of the *viscous limit* solution where $u = f(S^+)$ from Eq. (1.16). This implies that the downstream saturation is $S^+ = f^{-1}(u)$.
- At $x \in [0, x_0]$, the fourth order Runge–Kutta method is used successively to construct the solution backwards starting from the known point (x_0, S^+). To get S^- at the discontinuity, its relationship with S^+ is based on the continuity of capillary pressure at this point whereby:

$$p_c(\tau^-, S^-) = p_c(\tau^+, S^+) \Rightarrow S^- = J^{-1}\left(\frac{J^+}{\tau_r}\right) \tag{2.12}$$

where $\tau_r = \frac{\tau^+}{\tau^-}$ is the capillary variable ratio. The Runge–Kutta method employed here has a global truncation error of $O(h^4)$. At the left neighbourhood of the discontinuity, the slope field gets steeper with decreasing capillary number or as $h(S) \to 0$ when $S \to 0, 1$. In this case, the choice of Δx is adaptive to get the desired accuracy.

3 Results

3.1 Ascending $\tau(x)$

For the ascending case, we choose $\tau^- = 1$ and $\tau^+ = 2$. The capillary variable profile is plotted in Fig. 2. The resulting saturation and capillary pressure profiles are plotted in Fig. 2 for the purpose of quality control for the numerical scheme. For this purpose, we assume $u = 0.75$, $\gamma = 1$ and BC model for the J-function.

It is evident from Fig. 2 that the ascending case results in a water retention, the dashed black curve, compared with the viscous limit saturation solution, the solid magenta line. Note that the retention occurs upstream of the discontinuity and $S \to S_v$ as $x \to -\infty$. The reason behind this behaviour is based on the *capillary pressure postulate*. 'Given that the solution approaches the viscous limit from either side of the discontinuity, then the only possible way for the water phase to flow from higher $p_c(\tau^-, S)$ to lower $p_c(\tau^+, S)$ through the discontinuity is to *build up* in the vicinity upstream of the discontinuity in accordance with the continuity of the capillary pressure' (Yortsos and Chang 1990). The effect of saturation build-up is the gradual reduction in $p_c(\tau^-, S)$, by definition, until it reaches $p_c(\tau^+, S^-)$ at the discontinuity where $p_c(\tau^-, S^-) = p_c(\tau^+, S^+)$ as in Fig. 2.

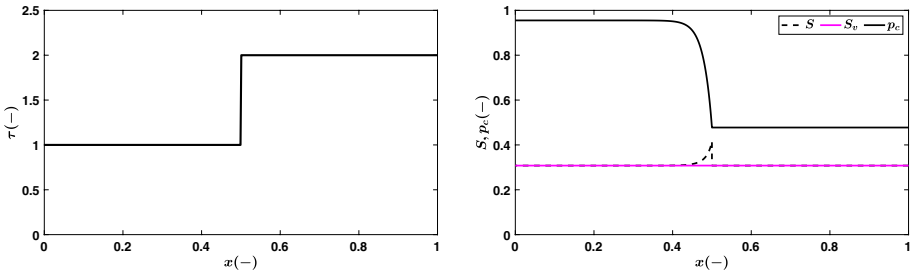

(a) Ascending $\tau(x)$ **(b)** $S_v(x)$, $S(x)$ and $p_c(x)$

Fig. 2 (**a**) Ascending capillary variable. (**b**) The resulting saturation and capillary pressure profiles at $u = 0.75$ and $\gamma = 1$

The geometric interpretation of the saturation build-up and the reduction in the capillary pressure upstream of the discontinuity is easily understood from the $p_c(\tau^-, S)$ and $p_c(\tau^+, S)$ curves plotted in the $p_c - S$ plane in Fig. 3.

As the water phase flows from left to right, the saturation increases from S_v to S^- at x_0^- and the path AB, the solid red line, is traversed along $p_c(\tau^-, S)$ curve. Then, it exhibits a discontinuity when flowing from x_0^- to x_0^+. This is translated in Fig. 3 as a horizontal jump from B to C, dashed red line, in accordance with the continuity of the capillary pressure postulate. Note that the points A and C are vertically aligned, which suggests that the build-up effect of saturation does not reach the boundary at $x = 0$. However, the build-up effect may reach the boundary for high capillary number, in which the points A and C will no longer be vertically aligned.

Now we revert to the capillary retention. Figure 4 shows the water capillary retention calculated using (2.1) against the capillary number for various fractional flow values. Each curve is characterized by three main regions depending on the *flow regime*: two plateaus that occur at lower and higher capillary numbers and a transition zone at intermediate capillary numbers. The plateaus are referred to as the *viscous* and *capillary* regimes, respectively, whereas the transition zone is referred as *viscous-capillary* regime. Figure 5 shows two saturation profiles nearly at these plateaus. Note in Fig. 5 how the saturation profile is behaving like a Heaviside function at the capillary regime. It is interesting to see how the transition zone for the curve $u = 0.001$ occurs at a relatively lower capillary number compared with the other three curves.

In Fig. 4, the key observation is related to the capillary retention for various fractional flow values as $\gamma \to \infty$ denoted by $\kappa_\infty = \kappa(u, \infty)$. The capillary retention at this limit increases with increasing fractional flow and then decreases which suggests the existence of a maximum in the range $u = (0.75, 0.999)$ by observation. This non-monotonic behaviour can be explained with the aid of Figs. 3 and 5. At the capillary regime, the saturation profile is constant in the upstream segment and that occurs at constant capillary pressure, the dashed red line in Fig. 3. The solid red line is not traversed. This means that $\kappa_\infty = S^- - S^+$, by definition. By observation, it seems that the *horizontal gap* between the two capillary pressure curves at constant capillary pressure is non-monotonic with capillary pressure.

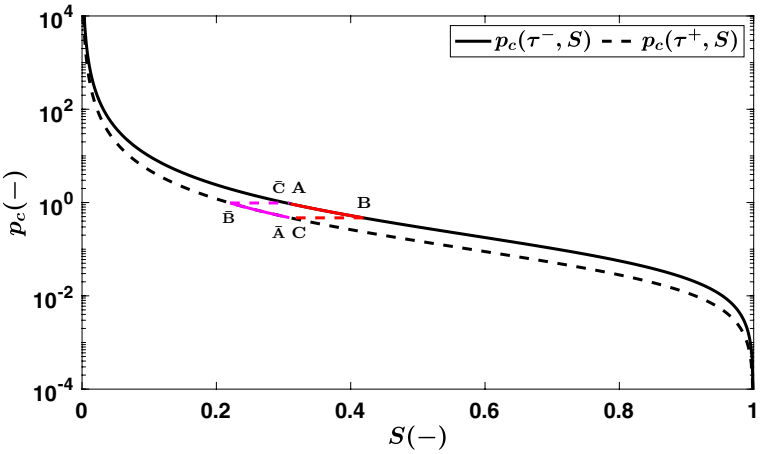

Fig. 3 Capillary pressure curves against water saturation for the upstream and downstream capillary variable

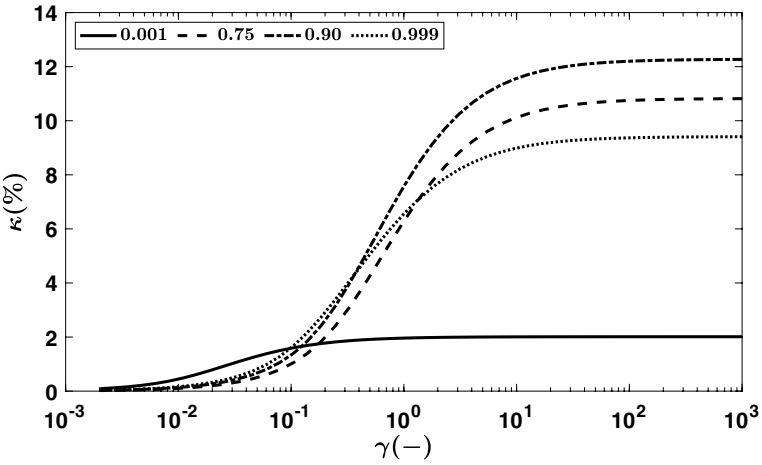

Fig. 4 Capillary retention against capillary number for various fractional flow values

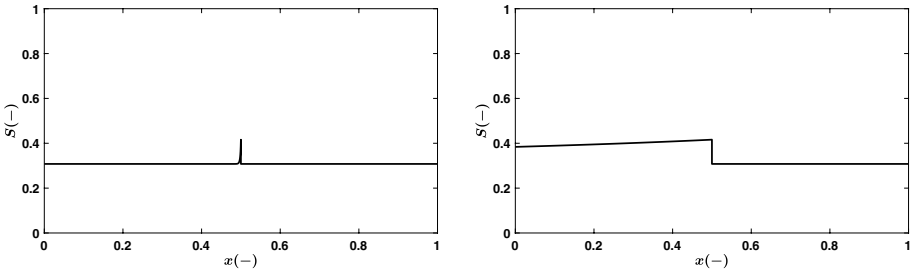

(a) $S(x)$ at $\gamma = 1 \times 10^{-2}$ and $u = 0.75$ **(b)** $S(x)$ at $\gamma = 1 \times 10^{2}$ and $u = 0.75$

Fig. 5 Saturation profiles at low and high capillary numbers

This also suggests that the existence of a maximum retention, denoted by κ^s_∞, is even more attractive. To find κ^s_∞, we define κ_∞ as:

$$\kappa_\infty = p_c^{-1}(\tau^-, p_c) - p_c^{-1}(\tau^+, p_c) \tag{3.1}$$

where p_c^{-1} is the inverse of the capillary pressure function. For our particular case where J is defined by Eq. (2.3), the function takes the form:

$$\kappa_\infty = \left(\left(q\tau^- p_c\right)^n + 1\right)^{-m} - \left(\left(q\tau^+ p_c\right)^n + 1\right)^{-m}. \tag{3.2}$$

Figure 6 shows the capillary limit retention against the capillary pressure. The maximum is roughly $\kappa^s_\infty = 0.13$ which occurs at $p^s_c = 0.14$. Note how $\kappa_\infty \to 0$ as $p_c \to 0, \infty$.

Figure 7 shows the capillary retention against the fractional flow for various capillary numbers. The retention increases with increasing capillary number, as expected. Note the existence of many maxima which are not in the capillary limit. However, these are lower than the maximum possible retention, κ^s_∞, estimated in Fig. 6. Also, these maxima seem

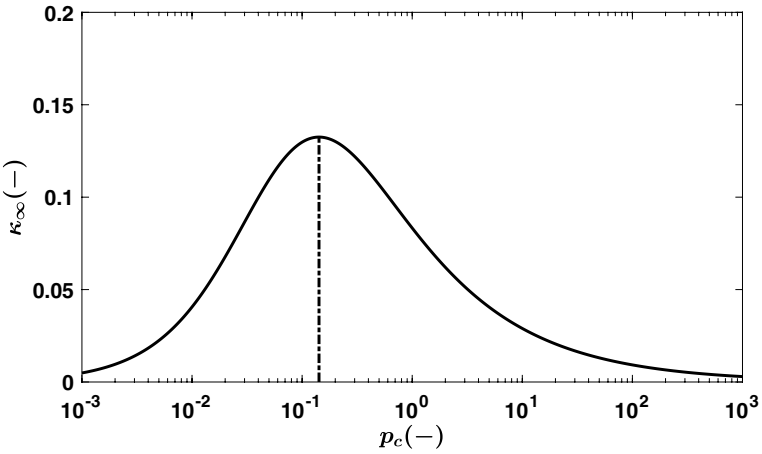

Fig. 6 The capillary limit retention against the capillary pressure

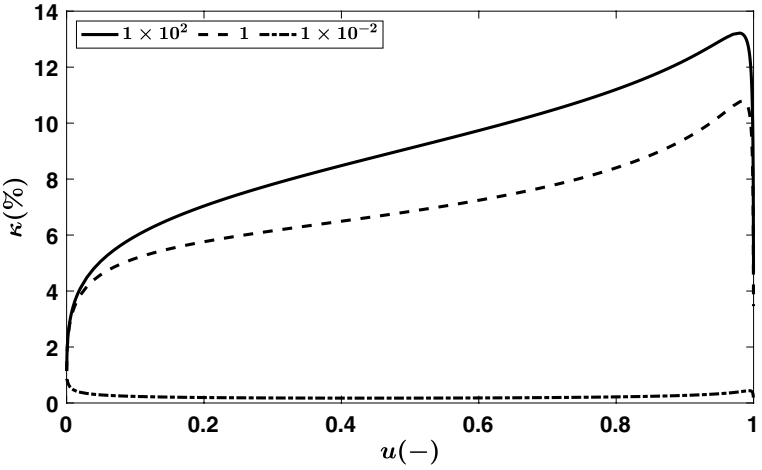

Fig. 7 Capillary retention against fractional flow for various capillary numbers

to migrate to lower fractional flow with increasing capillary number. Another important observation is related to the curve with $\gamma = 1 \times 10^{-2}$ where the local maximum occurring at higher u is roughly lower than the local maximum occurring at lower u. Whether these curves are influenced by the boundary $x = 0$ at which we restrict our evaluation for the capillary retention (Eq. 2.1) remains an open question.

The limits of capillary retention as $u \to 0, 1$ are quite subtle since we have truncated u near 0 and 1 for numerical stability purposes. However, we can argue that $\kappa \to 0$ as $u \to 1$. First note that $S^+ \leq S(x) \leq 1$, i.e. bounded, for the ascending case. As $u \to 1$, $S^+ \to 1$ which implies that $\kappa \to 0$, by definition, regardless of the flow regime. The same argument can be made for the case where $u \to 0$ which results in $\kappa \to 0$.

It is important, however, to note that the above limits are correct if capillary pressure curves coincide as $S_v \to 0, 1$, see Fig. 3. These types of capillary pressure curves are called

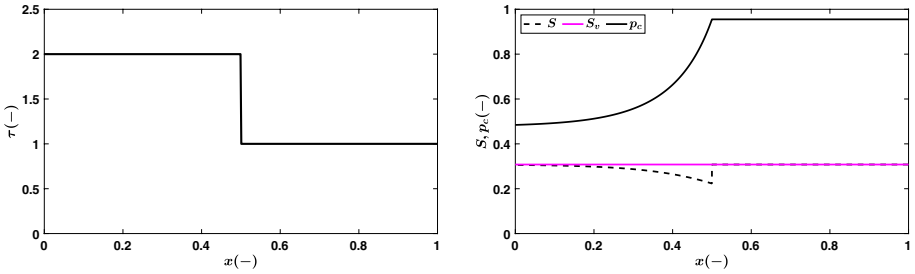

(a) Descending $\tau(x)$ **(b)** $S_v(x)$, $S(x)$ and $p_c(x)$

Fig. 8 (**a**) Descending capillary variable profile. (**b**) The resulting saturation and capillary pressure profiles at $u = 0.75$ and $\gamma = 1$

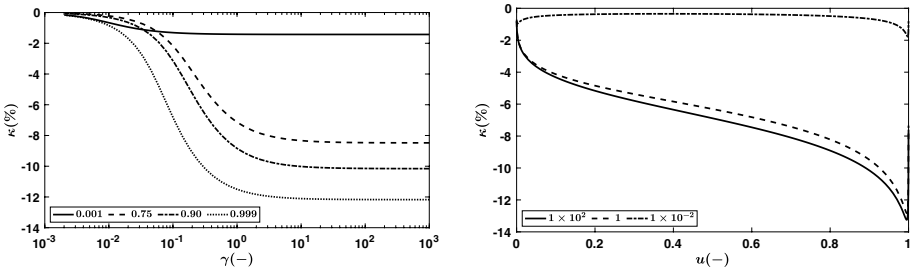

(a) κ vs γ for various u **(b)** κ vs u for various γ

Fig. 9 (**a**) Capillary retention against capillary number. (**b**) Capillary retention against fractional flow

'class I' in Van Duijn's classification (Duijn et al. 1995). Other classes have the feature where the capillary pressure curves do not coincide from one end or both ends. The continuity of the capillary pressure implies that capillary retention limits for these classes do not approach zero from one or both ends. As a result, the capillary retention might occur for these classes.

3.2 Descending $\tau(x)$

The descending case is obtained from (2.5) by letting $\tau^- = 2$ and $\tau^+ = 1$. The resulting τ is plotted in Fig. 8 . Figure 8 shows the resulting saturation and capillary pressure profiles. Compared to the ascending case, it is evident that the converse occurs in agreement with the continuity of the capillary pressure. For the water phase to flow from lower to higher capillary pressure values, its saturation must decrease as it approaches the discontinuity. See the traversed path $\bar{A}\bar{B}\bar{C}$, in Fig. 3. This yields an oil retention compared to the viscous limit saturation solution, the solid magenta line.

Regarding the capillary retention plots in Fig. 9, similar behaviours are encountered. In particular, the maximum retention at the capillary regime is similar to that of the ascending case, i.e. 13% which occurs at fractional flow of $u = f(S^+_{desc}) = f(S^-_{asc}) = 0.99$. This means that the curve $\kappa(u = 0.999)$ in Fig. 9 is already in a descending phase. The previous discussion regarding the capillary limits as $u \to 0, 1$ in the ascending case also applies to this case since we are using the same capillary pressure curves.

3.3 The Properties of κ^s_∞

The most important feature of κ^s_∞ is related to the boundedness of the capillary retention $\kappa(u,\gamma)$ for given J-curve with $\lim_{S_w\to 0} J = +\infty$ and $J(1) = 0$. By inspecting (2.2), one can deduce that

$$0 \le \kappa(u,\gamma) \le \kappa^s_\infty \tag{3.3}$$

for water retention. So κ^s_∞ acts as an *upper bound* for κ. For oil retention, it is a lower bound but we will use the term, upper, in absolute sense for both types of retention. It is desirable to understand the behaviour of this bound with respect to the capillary variable ratio, and the J-function. We put Eq. (3.2) in the following form:

$$\kappa^s_\infty(\tau_r, p^s_c) = \left(\left(q\tau^- p^s_c\right)^n + 1\right)^{-m} - \left(\left(q\tau^- \tau_r p^s_c\right)^n + 1\right)^{-m} \tag{3.4}$$

where $m, n > 0$. We allow τ_r, positive, to be a function of τ^+ only. Taking the derivative with respect to τ yields:

$$\frac{\partial \kappa^s_\infty}{\partial \tau_r} = mn\left(q\tau^- p^s_c\right)^n \frac{\tau^{n-1}}{\left(\left(q\tau^- \tau_r p^s_c\right)^n + 1\right)^{-(m+1)}} > 0. \tag{3.5}$$

This shows that κ^s_∞ is an increasing monotone with τ_r. To find κ^s_∞ and p^s_c for given τ_r where J is defined by (2.4), we put $\frac{\partial \kappa^s_\infty}{\partial p^s_c} = 0$ in (3.4) giving:

$$p^s_c = \frac{1}{q\tau_r^-}\left(\frac{1 - \tau_r^{\frac{n}{m+1}}}{\tau_r^{\frac{n}{m+1}} - \tau_r{}^n}\right)^{\frac{1}{n}} \tag{3.6}$$

and

$$\kappa^s_\infty = \left(\frac{\tau_r^n - \tau_r^{\frac{n}{m+1}}}{\tau_r^n - 1}\right)^m - \left(\frac{\tau_r^{\frac{nm}{m+1}} - 1}{\tau_r^n - 1}\right)^m. \tag{3.7}$$

It is interesting how κ^s_∞ is invariant under the scaling of J-curve by q. However, the location of this upper bound with respect to p^s_c is altered. For instance, in view of the capillary pressure curves in Fig. 3 for BC model. Increasing q by a factor of 10 will translate the two curves downwards by a factor of 10. Thus, the upper bound is unchanged whereas the capillary pressures will decrease by a factor of 10. Also, by substituting τ_r^{-1} in Eq. (3.7), one can show that:

$$\kappa^s_\infty\left(\frac{1}{\tau_r}\right) = \kappa^s_\infty(\tau_r). \tag{3.8}$$

This agrees with the previous numerical result, which showed that the upper bound is invariant under interchanging τ^- and τ^+. The only difference is that $u^s_{asc} < u^s_{desc}$.

To study the nonlinearity effect of the BC and VB models on the upper bound, one can study Eq. (3.6) with the view that m, $n(m)$ are variables. We prefer to study this schematically and we take the ascending case for this purpose. Figure 10 shows plots of two sets of capillary pressure curves. The plots with the black colour are the

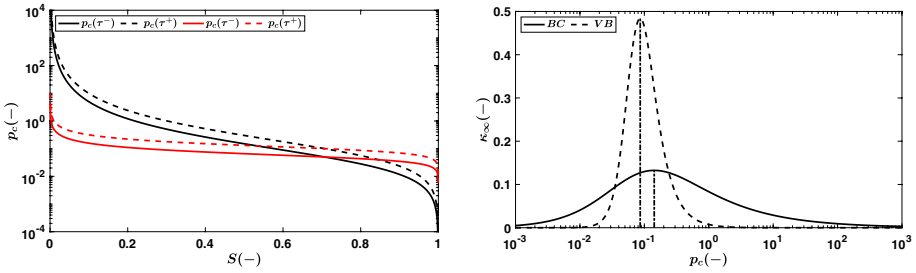

(a) $p_c(S)$ for BC and VB models **(b)** $\Delta S(p_c)$ for BC and VB models

Fig. 10 The capillary pressures and saturation differences for the BC and VB models

previous BC capillary pressures, and we have added the VB capillary pressures with $n(m = \frac{1}{2}) = 4$, shown in red, for the same capillary variable ratio. The vertical gaps, at particular saturation, between the BC and the VB curves are controlled by τ and, thus, they are relatively similar.

However, the horizontal gap is significantly different due to the flattening behaviour of the VB model for a wider range of saturation and lower range of capillary pressure. This, generally, requires a rapid change in the sign of curvature of the curve, which is the main cause of inflection points. This, indeed, happens to the VB model which exhibits an inflexion point at $S^s = \left(\frac{mn+1}{mn+n}\right)^m = 0.71$.

Figure 10 shows the capillary limit retention,κ_∞ for the two models along with the highlighted upper bounds, κ_∞^s. The VB's bound is 0.48, almost 3.7 times higher than the BC's bound.

To see how the upper bound change with the pore size distribution, we plot the capillary retention as a function of p_c and m for both models in Fig. 11. It is evident that at very low m, the bound is also very low and occurs at high capillary pressure for both models. However, with increasing m, the bound for the BC model increases gradually, whereas for the VB model increases rapidly and almost linearly. This behaviour in the upper bound with increasing m occurs at roughly constant capillary pressure. The curves at $m = \frac{1}{2}$ are those plotted in Fig. 10b and drawn here for reference. Observe the size of the window (capillary pressure range) in which the upper bound occurs for both models. The window is larger for the BC model and lower for the VB model, which is also clear from the curves drawn in Fig. 10.

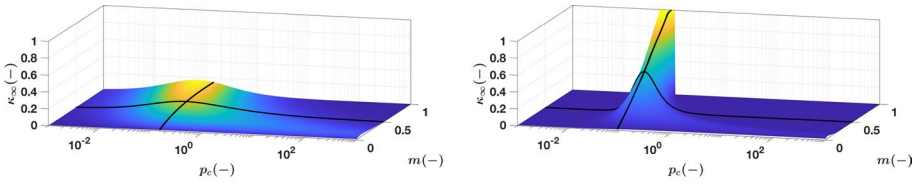

(a) $\Delta S(p_c, m)$ for BC model **(b)** $\Delta S(p_c, m)$ for VB model

Fig. 11 The saturation difference against capillary pressure and m for BC and VB models

4 Discussion

Capillary force in one-dimensional porous medium is responsible for many capillary-related phenomena. In the context of Buckley–Leverett displacement, it can smear the shock and the resulting capillary length relative to the Buckley–Leverett displacement grows with time (Buckley and Leverett 1942). It is also the cause of capillary end-effect in steady state, water-wet core experiments (Rapoport and Leas 1953; Kyte and Rapoport 1958; Johnson et al. 1959). Another phenomenon is related to heterogeneously discontinuous medium operating at the sub-meter scale which may have a major impact in oil recovery.

When two immiscible fluids flow simultaneously from a fine to a coarse sandstone medium, the capillary effect causes extra possession of water in the fine medium relative to the case that would occur if the capillary effect was absent or negligible (Fig. 2). This flow behaviour is governed by the continuity of capillary pressure. The fine medium has high capillary pressure and the coarse medium has low capillary pressure, so the fine medium capillary pressure has to decrease, i.e. increase in water saturation, to be continuous with the coarse medium capillary pressure. The opposite will occur if the fluid flow from a coarse to a fine medium, i.e. extra possession of oil (Fig. 9).

The continuation of the capillary pressure along the medium causes a saturation jump or step at the medium interface. This saturation jump is a function of fractional flow, capillary variable ratio, and the functional form of the Leverett *J*-curve.

The average saturation of the phase retained behind the medium interface, the so-called capillary retention, can be used to infer about the flow regime. The flow is near the viscous regime if there is low retention and it is near the capillary regime if there is high retention (Fig. 5). The three typical regimes are identified. The two plateaus occurring at low and high capillary numbers are the viscous and capillary regimes, respectively. The former regime has negligible retention and the latter has a maximum retention for a given fractional flow. The third regime is a transition between the viscous and capillary regimes, and occurs at intermediate capillary numbers (Fig. 4). One of the main findings is that the flow regime is not only a function of the capillary number but also the fractional flow.

The retention, in general, is difficult to characterize since it primarily depends on nonlinear saturation-dependent functions, i.e. the viscous limit fractional flow and the diffusivity functions. Nevertheless, we consider bounding this regime by a critical retention value that could occur for a given *J*-curve. The critical retention, named the upper bound, is the capillary limit retention that occurs for critical fractional flow value and corresponds to a maximum horizontal separation in the capillary pressure curve plot (Fig. 3). Then, this bound acts as an indicator and it is very useful in considering if the retention phenomenon matters or not. As the results show, the bound increases with increasing the capillary variable ratio across the medium interface, i.e. heterogeneity difference, and the form of the *J*-curve. For the latter one and a given capillary variable ratio, it was shown that the steeper *J*-curve has a lower bound than the flatter *J*-curve. For the purpose of demonstration, we take two models for the steeper and flatter cases and this is illustrated in Fig. 10.

5 Implications to Reservoir-Scale Recovery

More care is needed when discussing the potential implications of the current analysis to the field-scale oil recovery. Although the analysis is very restrictive, some field-scale implications are possible.

Various sedimentary structures can cause capillary retention including the cross beds, the most common structures found in sandstone reservoirs (van Lingen and Knight 1997). In such reservoirs, the displacement geometry is approximately linear provided that the dimensionless $R = \frac{L}{H}\sqrt{\frac{k_z}{k_x}} > 10$, where $\frac{L}{H}$ and $\sqrt{\frac{k_z}{k_x}}$ are the vertical reservoir aspect ratio and anisotropic ratio, respectively (Yortsos 1995). The displacement process is transient, Buckley–Leverett like, augmented by viscous instability at the early stage of the production phase. This displacement character is true even if the reservoir is ideally homogeneous, especially in viscous oil reservoirs, (Seright 2010). The presence of heterogeneity with various length scales, lithologies, and configurations complicates the displacement pattern even further.

However, in the view of the current analysis, the local displacement at the sub-meter scale at an instant in time can be approximated by the steady-state formalism. The effect of the time dimension is to change the fractional flow. This, in turn, changes the saturation profile and, hence, the capillary retention. Note that the upper bound for capillary retention identified here is independent of the fractional flow, and capillary number and hence can be used for transient processes. Various flow directions are possible, and the worst-case retention scenario occurs when the flow is across the heterogeneities. In the case of steeper *J*-curves with low to moderate random capillary variable ratios, the upper bound is minimal regardless of the various lithologies and their configurations. The random heterogeneity assumption is essential so that the capillary retention of a particular phase does not accumulate when averaged over the entire reservoir. In such conditions, the upper bound can be used to assert the insignificance of the field-scale capillary retention. We conjecture that this conclusion may not hold at high capillary variable ratios which are a subject of further investigation.

6 Conclusion

In a more relaxed and general setting, the capillary retention in a porous medium with a single discontinuity depends on the phase mobilities and Leverett *J*-curves, end-point mobility ratio, capillary number, fractional flow, capillary variable. If the retention is only function of the capillary number and fractional flow, then three retention regions are identified which are related to the flow regime. The first region is the capillary regime at high capillary numbers in which the highest retention occurs for given fractional flow. The second is the viscous regime at high capillary numbers in which the retention is negligible regardless of the fractional flow. The third region is the transition between the capillary and viscous regimes, which, in general, occurs at intermediate capillary numbers. It is demonstrated that the middle transition zone does not occur at a particular capillary number. Moreover, the position and width of the zone are not fixed but depend on the fractional flow.

Key to the analysis is the identification of the upper bound for the capillary retention. This is defined as the capillary limit retention where the difference in the upstream and downstream saturation is maximum. It depends on the capillary variable ratio τ and the form of the J-curve but invariant under the linear scaling of the *J*-curve or the order of heterogeneity. Finally, it was demonstrated that the Van Genuchten–Burdine model has a higher bound than that of the Brooks–Corey model. This is mainly due to the flattening feature of the capillary pressure curves at intermediate saturation.

In the case of steeper *J*-curves with low to moderate random capillary variable ratios, the upper bound is minimal regardless of the various lithologies and their configurations. In such conditions, the upper bound can be used to assert the insignificance of the field-scale capillary retention.

Acknowledgements The authors thank Petroleum Development Oman (PDO) for funding the research in the Institute of Geoenergy (IGE) at Heriot-Watt University.

Funding The research was funded by Petroleum Development Oman (PDO).

Data Availability Data and materials are accessible and were uploaded as supplementary material.

Declarations

Conflict of interest We wish to confirm that there are no known conflicts of interest associated with this research and there has been no significant financial support for this work that could have influenced its outcome.

References

Amaefule, J.O., Altunbay, M., Tiab, D., Kersey, D.G., Keelan, D.K.: Enhanced reservoir description: Using core and log data to identify hydraulic (flow) units and predict permeability in uncored intervals/wells. All Days, SPE. (1993). https://doi.org/10.2118/26436-ms

Bear, J.: Dynamics of fluids in porous media. Soil Sci. **120**(2), 162–163 (1975). https://doi.org/10.1097/00010694-197508000-00022

Blunt, M.J.: Multiphase Flow in Permeable Media. Cambridge University Press (2017). https://doi.org/10.1017/9781316145098

Bramwell, M.C., Kreyszig, E.: Introductory functional analysis with applications. Math. Gaz. **63**(424), 137 (1979). https://doi.org/10.2307/3616033

Brooks, R.H., Corey, A.T.: Properties of porous media affecting fluid flow. J. Irrig. Drain. Div. **92**(2), 61–88 (1966). https://doi.org/10.1061/jrcea4.0000425

Buckley, S., Leverett, M.: Mechanism of fluid displacement in sands. Trans. AIME **146**(01), 107–116 (1942). https://doi.org/10.2118/942107-g

Carman, P.: Fluid flow through granular beds. Chem. Eng. Res. Des. **75**, S32–S48 (1937). https://doi.org/10.1016/s0263-8762(97)80003-2

Chang, J., Yortsos, Y.C.: Effect of capillary heterogeneity on buckley-leverett displacement. SPE Reserv. Eng. **7**(02), 285–293 (1992). https://doi.org/10.2118/18798-pa

Coates, G. R., Dumanoir, J.: A new approach to improved log-derived permeability, *All Days*, SPWLA Annual Logging Symposium (1973)

Dale, M., Ekrann, S., Mykkeltveit, J. Virnovsky, G.: Effective relative permeabilities and capillary pressure for 1d heterogeneous media, ECMOR IV - 4th European Conference on the Mathematics of Oil Recovery, European Association of Geoscientists and Engineers. https://doi.org/10.3997/2214-4609.201411163 (1994)

Debbabi, Y., Jackson, M.D., Hampson, G.J., Salinas, P.: Capillary heterogeneity trapping and crossflow in layered porous media. Transp. Porous Media **120**(1), 183–206 (2017). https://doi.org/10.1007/s11242-017-0915-z

Duijn, C.J.V., Molenaar, J., Neef, M.J.D.: The effect of capillary forces on immiscible two-phase flow in heterogeneous porous media. Transp. Porous Media **21**(1), 71–93 (1995). https://doi.org/10.1007/bf00615335
Ekrann, S., Dale, M., Langaas, K., Mykkeltveit, J.: Capillary limit effective two-phase properties for 3d media. All Days, SPE. (1996). https://doi.org/10.2118/35493-ms
Howlett, J., Henrici, P.: Elements of numerical analysis. Math. Gaz. **50**(373), 357 (1966). https://doi.org/10.2307/3614752
Johnson, E., Bossler, D., Bossler, V.N.: Calculation of relative permeability from displacement experiments. Trans. AIME **216**(01), 370–372 (1959). https://doi.org/10.2118/1023-g
Kozeny, J.: Uber kapillare leitung der wasser in boden, Royal Academy of Science, Vienna. Proc. Class I **136**, 271–306 (1927)
Kyte, J., Rapoport, L.: Linear waterflood behavior and end effects in water-wet porous media. J. Petrol. Technol. **10**(10), 47–50 (1958). https://doi.org/10.2118/929-g
Ledeboer, R.: Capillary entrapment in small scale heterogeneous porous media, Technical report, Faculty of Mining and Petroleum Engineering,Delft University of Technology (1992)
Leverett, M., Lewis, W., True, M.: Dimensional-model studies of oil-field behavior. Trans. AIME **146**(01), 175–193 (1942). https://doi.org/10.2118/942175-g
Miall, A.D.: Fluvial styles and facies models, The Geology of Fluvial Deposits, Springer Berlin Heidelberg, pp. 191–249. https://doi.org/10.1007/978-3-662-03237-4-8 (2006)
Rapoport, L., Leas, W.: Properties of linear waterfloods. J. Petrol. Technol. **5**(05), 139–148 (1953). https://doi.org/10.2118/213-g
Reading, H.G.: Sedimentary environments: processes, facies and stratigraphy. John Wiley and Sons (2009)
Seright, R.S.: Potential for polymer flooding reservoirs with viscous oils. SPE Reserv. Eval. Eng. **13**(04), 730–740 (2010). https://doi.org/10.2118/129899-pa
Timur, A.: An investigation of permeability, porosity, and residual water saturation relationships for sandstone reservoirs. The Log Anal.**9**(04) (1968)
Tixier, M.: Evaluation of permeability from electric-log resistivity gradients. The Oil Gas J. **16**, 113–133 (1949)
van Duijn, C., de Neef, M.: Similarity solution for capillary redistribution of two phases in a porous medium with a single discontinuity. Adv. Water Resour. **21**(6), 451–461 (1998). https://doi.org/10.1016/s0309-1708(97)00012-2
van Genuchten, M.T.: A closed-form equation for predicting the hydraulic conductivity of unsaturated soils. Soil Sci. Soc. Am. J. **44**(5), 892–898 (1980). https://doi.org/10.2136/sssaj1980.03615995004400050002x
van Lingen, P., Knight, S.: Evaluation of Capillary Entrapment within Reservoir Flow Units, All Days. Society of Petroleum Engineers (SPE) (1997). https://doi.org/10.2118/38934-MS
Wyllie, M., Rose, W.D.: Some theoretical considerations related to the quantitative evaluation of the physical characteristics of reservoir rock from electrical log data. J. Petrol. Technol. **2**(04), 105–118 (1950). https://doi.org/10.2118/950105-g
Yortsos, Y.C.: A theoretical analysis of vertical flow equilibrium. Transp. Porous Media **18**(2), 107–129 (1995). https://doi.org/10.1007/bf01064674
Yortsos, Y.C., Chang, J.: Capillary effects in steady-state flow in heterogeneous cores. Transp. Porous Media **5**(4), 399–420 (1990). https://doi.org/10.1007/bf01141993

Authors and Affiliations

Al Yaqathan Al Ghafri[1] · Eric Mackay[1] · Karl Stephen[1]

✉ Al Yaqathan Al Ghafri
asa19@hw.ac.uk

[1] Institute of Geoenergy Engineering (IGE), Heriot-Watt University, Riccarton, Edinburgh EH14 4AS, Scotland